THE ASTROPHYSICAL JOURNAL, 419:94–103, 1993 December 10

H I SPIN TEMPERATURES AND HEATING REQUIREMENTS IN OUTER REGIONS OF DISK GALAXIES

EDVIGE CORBELLI[1]
Osservatorio Astrofisico di Arcetri, Largo E. Fermi 5, 50125 Firenze, Italy
AND
EDWIN E. SALPETER[2]
Center for Radiophysics and Space Research, Space Sciences Building, Cornell University, Ithaca, NY 14853
Received 1992 December 28; accepted 1993 June 18

ABSTRACT

We show how to use 21 cm emission and absorption studies to estimate the heat inputs to the neutral gas in low pressure environments, such as in outer disks of spiral galaxies, in galactic halos or in intergalactic space. For a range of model parameters we calculate the gas kinetic and spin temperatures (T_K and T_S) and the relation between T_S and the heat input to the gas. We outline the conditions for a "two-phase medium" to exist. We find that although T_S can be much smaller than T_K, T_S is always $\gg 3$ K for column densities greater than 5×10^{18} cm^{-2}. This excludes the possibility that relevant H I masses at the periphery of galaxies are invisible at 21 cm in emission. Therefore sharp H I edges, observed in outer disks near column densities $N_l \sim 2 \times 10^{19}$ cm^{-2}, cannot be "fictitious" edges due to a sudden decrease of the 21 cm brightness. The outermost interstellar gas in a disk galaxy is more directly affected by external processes, and in this paper we estimate the intensity of the extragalactic background at energies close to 0.1 keV by comparing our theoretical results with H I emission/absorption studies. We take into account the possibility that some energy produced in the inner regions affects the energy balance in outer regions. We find that in the absence of any other local heat source QSO-dominated background models are still compatible with the spin temperature limits derived for the two best documented H I emission/absorption studies in outer regions. However, if future observations should establish that the spin temperature is as high as 1000 K, then relevant energy inputs from local sources become necessary.

Subject headings: galaxies: ISM — radio lines: galaxies

1. INTRODUCTION

Neutral hydrogen exists outside the stellar region of spiral galaxies as extended disks, coplanar or tilted with respect to the innermost luminous disk. Isolated concentrations, clouds or plumes have sometimes been detected well outside the H I disk (see for example Giovanelli & Haynes 1988 for a review). These blobs may indicate a recent disturbance in the H I distribution due to tidal interactions with a companion or to a strong burst of activity in the inner disk. In our Galaxy smaller blobs of H I, closer to the luminous disk, and known as high velocity clouds (HVCs), have also been detected (Giovanelli 1980).

The physical conditions of the gas in the outer regions of spiral galaxies are not constrained as they are in the interstellar medium. In the inner disk of our Galaxy, where star formation takes place, the following conditions hold: (1) neutral hydrogen column densities are of order $N_{\rm H\,I} \sim 2 \times 10^{20}$–$10^{21}$ cm^{-2}, and extragalactic UV or soft X-ray photons with energies between 13.6 and 200 eV hardly penetrate this layer; (2) even without magnetic pressure and bulk motion ram pressure, the gas thermal pressure is fairly large, $P/k \sim 3000$ cm^{-3} K (k is the Boltzmann constant); (3) neutral hydrogen exists in a cold phase at the kinetic temperature $T_K \sim 80$ and in a warm phase at $T_K \sim 8000$ K which fills a nontrivial part of our ISM ($\geq 30\%$ Brinks 1990; Knapp 1990). The ionization of the gas in the midplane might be due to O and B starlight (Kulkarni & Heiles 1988), and the mechanical energy input to the gas from O star winds and from blast-waves produced by supernovae (McKee & Ostriker 1977). However, these hot stars cannot easily account for the diffuse warm component observed at a few hundreds parsecs above the Galactic midplane (Reynolds 1990).

In outer disks, or in high velocity clouds, stars are absent and the ionizing flux as well as the mechanical energy input, from the stellar disk of the galaxy, might be very small. If chains of supernovae feed galactic fountains which reach the halo directly (Heiles 1987; Corbelli & Salpeter 1988; MacLow & McCray 1988; Martin & Bowyer 1990) or if there is hydromagnetic wave dissipation (Ferriere, Zweibel, & Shull 1988) then the nonradiative energy input into the outer regions are important. Ionizing flux from extragalactic sources is likely to be present due to thermal free-free emission from hot gas, to quasars, or to more exotic sources like dark matter decay (Melott, McKay, & Ralston 1988; Sciama 1990) or hidden X-UV emitters. The far-UV and soft X-ray emission from quasars is of interest here because we mainly consider regions with $N_{\rm H\,I} \leq 5 \times 10^{19}$ cm^{-2} and photons below 0.2 keV, which do not affect the inner disk, penetrate these smaller column densities and give a large ionization rate. We do not discuss which ionizing fluxes and nonradiative heat inputs are more likely on physical grounds but we parameterize the overall ionizing flux and the nonradiative energy input separately and calculate their effects on the H I gas. Using H I observations we can then investigate indirectly the energetic environment of

[1] E-mail: edvige@arcetri.astro.it
[2] E-mail: hann@astrosun.tn.cornell.edu

spiral galaxies. The absence of stars in outer regions makes self-gravity of the gas layer an important force which has to be considered, together with dark matter and coronal gas, in equilibrium models. Nevertheless we expect a much lower thermal pressure than that measured in the inner disk, as suggested by the flaring of the outer disk observed in external galaxies and in our own Galaxy (Merrifield 1992).

H I absorption studies both on outer disks and on HVCs, show that only a very small fraction of the gas has low enough temperature to be detected in absorption (Corbelli & Schneider 1990, hereafter CS; Colgan, Salpeter, & Terzian 1990, hereafter CST; Wakker, Vijfschaft, & Schwarz 1991; Carilli, van Gorkom, & Stoke 1989; Carilli & van Gokom 1992; Schneider & Corbelli 1993). However, sensitive searches of H I emission at some locations where no absorption measurements are possible indicate that there is a transitional H I column density N_l such that appreciable emission is seen for $N_B \gtrsim N_l$ but little emission is seen for $N_B < N_l$. We use the symbol N_B to indicate the column density derived directly from the 21 cm brightness temperature; $N_B = N_{\rm H\,I}$ when T_S is well above the background radiation temperature, T_R, otherwise $N_B < N_{\rm H\,I}$. The transitional column density N_l is of the order of 5×10^{18} cm^{-2} for high-velocity clouds and is of the order of 2×10^{19} cm^{-2} for outer disks (CST; Corbelli, Schneider, & Salpeter 1989) or slightly smaller (Hoffman et al. 1993). In this paper we discuss (and then eliminate) the possibility that, due to low pressure conditions and to low photoionization rate in outer regions, when $N_{\rm H\,I}$ gets below N_l, the spin temperature strongly deviates from the gas kinetic temperature and, while T_S approaches T_R, N_B is depressed with respect to $N_{\rm H\,I}$. Fictitious H I edges would then appear if one assumes that $N_B \simeq N_{\rm H\,I}$. The lack of H I absorption lines in outer regions already suggests that "subthermal effects" cannot hide appreciable H I masses, but we shall show more quantitatively that subthermal effects are not responsible for H I edge appearances. A totally different possibility, and a likely explanation for H I edges, is that they are sharp H I–H II transitions due to some ionizing flux. This will be analyzed in detail by Corbelli & Salpeter (1993, hereafter Paper II). Nevertheless due to the uncertainties in the evaluation of H I masses in extragalactic objects where no absorption measures are possible (Giovanelli & Haynes 1991; Schneider et al. 1989) and also to the importance of subthermal effects for H I absorption lines, we shall present here a full calculation of the spin temperature for several heating inputs outside the galaxy.

In § 2 we introduce some models for the extragalactic soft X-ray background radiation, and in § 3 we display the equilibrium equations and parameters used for modeling the gas distribution outside the stellar disk. Section 4 shows results relative to subthermal effects in the 21 cm emission line, and in § 5 we derive in more generality the relation between the kinetic and spin temperature as a function of the backgrond radiation intensity and of additional nonionizing local heat sources. We outline the conditions of the H I in a low-density medium pervaded with decaying neutrinos in § 6. The last section summarizes constraints on the energetic environment of spiral galaxies which can be set by comparing our theoretical results with 21 cm observations.

2. LOCAL ENERGY INPUTS AND THE EXTRAGALACTIC SOFT X-RAY BACKGROUND

As discussed in the introduction, there may be energy inputs which are nonradiative and nonionizing and which may vary from one galaxy to another or from one region to another (tidal interaction, hydromagnetic wave heating, fountains, etc.). We shall characterize these inputs using a single number, E_{nr}, the heat per hydrogen atom per second due to nonphotoionizing sources in units of eV s^{-1}, which should be added to the heat input from ionizing radiation, E_r. The ionization-recombination equilibrium depends on the photon spectrum $N(E)$. Below we summarize the known upper or lower limits to the extragalactic background radiation at zero redshift and then we will parameterize various model assumptions.

The UV and soft X-ray background has been reviewed by Bowyer (1991) and by McCammon & Sanders (1990). Above $\sim$2 keV a uniform extragalactic X-ray flux of power-law form is known to exist (Schwartz 1978):

$$\frac{dN}{dE} = 7.7 E_{\rm keV}^{-1.4} \text{ photons cm}^{-2}\text{ s}^{-1}\text{ sr}^{-1}\text{ keV}^{-1}\,. \quad (1)$$

Between 2 and 0.5 keV the total X-ray background is about 3×10^{-8} ergs cm^{-2} s^{-1} sr^{-1} (Shanks et al. 1991; Wu et al. 1991), higher than an extrapolation of equation (1) to this energy range, but the extragalactic contribution is uncertain because of local emission, and it is not measurable directly at all below 0.3 keV because of absorption by the local H I disk. The space density and luminosity function for quasars are known for redshifts $z < 2$ (see, e.g., Hartwick & Schade 1990) and their contribution to the flux between 2 and 0.5 keV has been estimated. Preliminary analysis of *ROSAT* deep survey images shows that quasars can account for at least 20% of the measured X-ray background below 2 keV (Hasinger, Schmidt, & Trumper 1991; Wu & Anderson 1992), and therefore we consider 5×10^{-9} ergs cm^{-2} s^{-1} sr^{-1} as a definite lower limit for the extragalactic background intensity between 2 and 0.5 keV. An extrapolation of equation (1) down to 1.5 keV yields this minimum expected intensity which we consider in examining the possibility of strong subthermal effects in emission.

In this paper we use a few spectral models of the extragalatic background radiation down to 0.1 keV. If this background is dominated by quasars, its spectral shape in the absence of attenuation is approximately of the form

$$\frac{dN}{dE} = I \times E_{\rm keV}^{-2.4} \text{ photons cm}^{-2}\text{ s}^{-1}\text{ sr}^{-1}\text{ keV}^{-1}\,, \quad (2)$$

which we shall refer to as the "quasar spectrum." For $I \simeq 15$ the spectrum described by equation (2) corresponds to a flux density $\simeq 4 \times 10^{-23}(E_{\rm eV}/13.6)^{-1.4}$ ergs cm^{-2} s^{-1} sr^{-1} Hz^{-1}. This flux at zero redshift was suggested by Sargent et al. (1979) and connects the so called "blue bump," observed in QSO spectra, with the cosmic background flux observed above 2 keV. In a recent paper Madau (1992) estimates a lower value of the integrated UV cosmic background from observed QSOs. He takes into account the possible attenuation of the flux due to intervening Lyman-α clouds. However above 0.1 keV attenuation is probably unimportant and Madau's estimate of the unattenuated flux down to a cutoff energy of 0.1 keV is given by the quasar spectrum of equation (2) with $I \simeq 5$.

We shall consider three different cases for flux and energy inputs. For Case A we assume the minimum extragalactic X-ray flux in order to compute the most extreme subthermal effects. We use a more likely flux for Case B and Case C and show how to use H I spin temperature measurements to con-

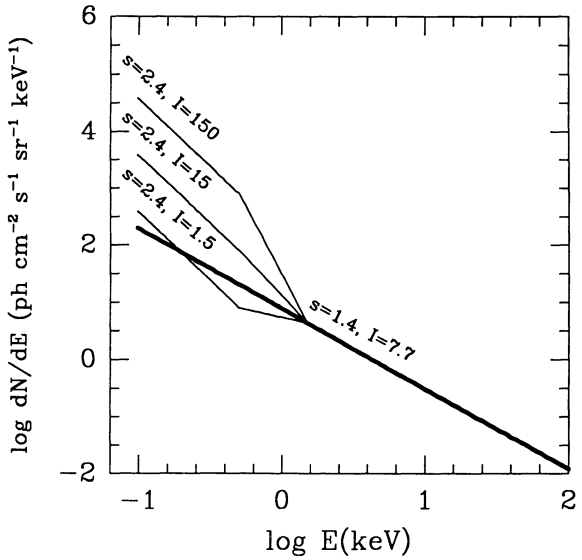

FIG. 1.—Some of the X-ray spectra used. At energies above 1.5 keV all the spectra have $s = 1.4$ $I = 7.7$, and the thick line shows this spectrum extended down to 0.1 keV as it has been used for Case B. The same spectrum has been used for Case A but with lower cutoff energies at 1.5 or 0.5 keV. All the other lines are examples of spectra used for Case C and are labeled according to the corresponding values of I and s (see eq. [3]).

strain the extragalactic background flux or the local heating just outside disk galaxies.

Case A.—We set $E_{nr} = 0$ and use the flux described by equation (1) with a lower cutoff energy $E_c = 1.5$ keV or $E_c = 0.5$ keV (in this last case about 60% of the observed background flux between 2 and 0.5 keV is of extragalactic origin).

Case B.—We consider $E_{nr} \neq 0$ as an adjustable parameter and use a low quasar flux, namely equation (1) with a cutoff energy $E_c = 0.1$ keV.

Case C.—We add a soft X-ray component in the energy range $E_c < E < 1.5$ keV, to the cosmic spectrum given by equation (1). The following form describes the spectral law which we use in this case:

$$\frac{dN}{dE} = \begin{cases} 7.7 \times E_{\rm keV}^{-1.4} & E \geq 1.5 \text{ keV} \\ A E_{\rm keV}^{-b} & 0.5 \leq E < 1.5 \text{ keV} \\ I E_{\rm keV}^{-s} & E_c \leq E < 0.5 \text{ keV} \\ 0 & E < E_c \end{cases}$$

$$\text{photons cm}^{-2}\ \text{s}^{-1}\ \text{sr}^{-1}\ \text{keV}^{-1}\,, \quad (3)$$

where A and b are constants determined by requiring dN/dE to be continuous at 0.5 and at 1.5 keV and I is an adjustable parameter. In this paper we use $E_c = 0.1$ keV, $s = 2.4$, and $E_{nr} = 0$ unless stated otherwise. The quasar spectrum in equation (2) can be represented to a good approximation by equation (3) using $s = 2.4$ (and $I \sim 5$ for Madau's intensity).

In Figure 1 we show dN/dE for some spectra used. The background spectrum at energies close to the Lyman limit will not be of interest in this paper because here we consider the heating of slabs with H I column densities $\gtrsim 0.5 \times 10^{19}$ cm^{-2}. However, the complete absence of photons below 0.1 keV is an oversimplification; some photons below 0.1 keV will penetrate the gas with low H I column density and increase the ionization rate slightly. In § 6 we discuss T_S and T_K for the case of monochromatic photons with $E \sim 14.5$ eV which are produced locally throughout the disk.

3. CHARACTERISTIC PARAMETERS OF H I GAS OUTSIDE A GALAXY

The brightness temperature of the 21 cm emission line, T_B, is related to the column density of neutral hydrogen along the line of sight, $N_{\rm H\,I}$:

$$T_B \propto N_B \equiv \chi_B N_{\rm H\,I}\,, \quad \chi_B \equiv \frac{T_S - T_R}{T_S}\,, \quad (4)$$

where $T_R = 2.73$ K is the temperature of the microwave background radiation, T_S is the spin temperature, defined through the population of the two hyperfine levels of neutral hydrogen (Field 1958). The factor χ_B is close to unity if the kinetic temperature, T_K, is well above the cosmic background temperature, and the medium is in LTE ($T_S \simeq T_K$). In this case the brightness temperature is directly proportional to $N_{\rm H\,I}$. The spin temperature is important for the optical depth at the line center τ_c which can be determined through absorption measurements

$$\tau_c = \frac{5.14 \times 10^{19}}{\omega} \frac{N_{\rm H\,I}}{T_S}\,, \quad (5)$$

where ω is the width of the line at half maximum in km s^{-1}. Most absorption and emission studies give T_S and $N_{\rm H\,I}$ and not the kinetic temperature of the medium because ω might not be proportional to $\sqrt{T_K}$, like if there is turbulence in the medium or the absorption line is unresolved. If ω is unknown we use the following value:

$$\omega \simeq \max\,(4,\ 0.21\sqrt{T_K})\ \text{km s}^{-1} \quad (6)$$

based on the line width of the few detected absorption lines (Rubin, Thonnard, & Ford 1982; Carilli & van Gorkom 1992). Deviations of T_S from T_K are especially important in outer regions where low densities slow down the collisional excitation of hyperfine levels of H. We calculate T_S for all cases in this paper using equation (15) of Field (1958). We consider Lyman-α pumping through photons generated by H^+–e recombinations (Spitzer 1978), by bound-bound transitions due to thermalized electrons (Spitzer 1978), by bound-bound transitions due to nonthermalized electrons coming from H photoionization (Shull & Van Steenberg 1985). Following Deguchi & Watson (1985) we set the Lyman-α temperature T_L equal to T_K and use the expression of Bonilha et al. (1979) for the number of Lyman-α photon scatters inside the cloud, disregarding the possibility of strong velocity gradients. For the collisional de-excitation probability of the hyperfine levels via neutral and ionized H atoms, and via electrons, we use the expression given by Smith (1966). For $T_R \ll T_S \ll T_K$ the gas is still far from thermodynamic equilibrium but the factor χ_B is very close to unity. This means that subthermal effects show up much more easily in absorption rather than in emission measures, because emission depends on the ratio between the population of the two hyperfine levels which remains $\simeq 3$. Absorption depends on their population difference which can vary by a much larger factor.

The gas will be considered distributed in a slab, with the vertical extension much smaller than the horizontal one. This is a good representation for extended H I disks or flat clouds in the outer parts of galaxies. For more spherical blobs our calculation will be indicative but not rigorously correct. The vertical distribution of gas density depends on the ratio of dark matter to gas and on any contribution of magnetic fields to pressure (or to buoyancy). These effects will be discussed in detail in Paper II; in this paper we assume that the ideal gas law con-

nects pressure, P, to gas kinetic temperature, T_K. Furthermore we shall use here the single slab approximation. For fixed values of the H I column density we compute the kinetic temperature and subthermal effects at a height $z = z_{1/2}$ above the central plane such that half the gas mass per unit area lies between $-z_{1/2}$ and $+z_{1/2}$. The attenuation of the extragalatic flux due to photoionization of H I, He I, and He II, is computed assuming that the fractional ionization of He I and He II at all levels is the same as at $z_{1/2}$.

The real pressure will have an additional term due to the external pressure, P_{ext}, and to the compression from a dark matter distribution. Charlton, Salpeter, & Hogan (1993) estimate that the purely extragalactic value for P_{ext}/k is less than ~ 4 cm^{-3} K but some galactic coronal gas is likely to increase the effective value of P_{ext}. For a spherical halo which gives a rotational velocity of 100 km s^{-1} at $R = 15$ kpc, the dark matter compression is equivalent to about 70 cm^{-3} K. Since in this paper we use the uniform slab approximation we mimic the effects of P_{ext}, dark matter, and eventually of some internal nonthermal pressure in one single term, P_0. We use the ideal gas law and we consider $0.1 \leq P_0/k \leq 500$ cm^{-3} K. The following expression describes the total pressure we use for a given column density of gas (see Spitzer 1942; Ibañez & di Sigalotti 1984):

$$\frac{P}{k} = \frac{P_0}{k} + \frac{P_{sg}}{k} \simeq \frac{P_0}{k} + \frac{\pi G m_H^2}{2.3k} N_{tot}^2 (1 + 4h_{He})^2$$
$$\simeq \frac{P_0}{k} + 0.36 \left(\frac{N_{tot}}{10^{19}} \right)^2 \text{ cm}^{-3} \text{ K} , \quad (7)$$

where G is the gravitational constant, m_H is the hydrogen mass, $h_{He} \simeq 0.1$ is the helium abundance relative to hydrogen, and N_{tot} is the total (H I + H II) hydrogen column density (i.e., twice the gas surface density above the equatorial plane).

We omit dust grains entirely and we assume that all elements heavier than He have only half the solar abundance (unless specified differently) and that there is enough UV light below 13.6 eV, from the background or scattered ouside the stellar disk, to keep most of the carbon, silicon, and iron singly ionized. For the range of pressures that we consider this is a good assumption (Bowyer 1991). Then the heating rate due to photoionization of C I does not depend on the UV photon intensity but only on the mean photon energy and we use the value $E_C = 2$ eV for the excess energy. In the temperature range that we consider ($T_R < T_K < 17{,}000$ K) cooling is dominated by collisional excitation of C II, Si II, Fe II by electrons and H I atoms at low temperatures, and by excitation of the $n = 2$ level of H I at higher temperatures. However cooling by free-free emission and by H II recombinations are considered as well. $P_0/k \geq 0.1$ ensures the recombination time for H II to be shorter than 10^{10} years.

For the ionization-recombination equilibrium of H I, He I, and He II we use the "on the spot approximation" with the photoionization cross section of H I, He I, and He II as given by Spitzer (1978) and Brown (1971). We assume that no photons escape from hydrogen recombinations to the $n = 1$ level (nor from helium recombinations to $n \geq 1$) because they are absorbed elsewhere by other H I atoms. Also, due to low volume densities in outer regions we can assume to a good approximation that all the He I and He II recombination photons are absorbed by H I atoms (Osterbrock 1989). We include secondary electrons, the heat, and the Lyman-α photons produced by primary electrons created via photoionization of H I, He I, and He II by using results of a Monte Carlo simulation (Shull & Van Steenberg 1985). No secondary electrons are considered when primary electrons are created via collisions with other atoms. This and the omission of collisional ionization of helium atoms are good assumptions since we consider only temperatures below 17,000 K. Unfortunately the complete set of results by Shull & Van Steenberg (1985) is given as function of the fractional ionization of H only for X-ray energies well above 0.1 keV. For lower energies they show the fractional energy deposited as heat and the number of secondary electrons ejected from hydrogen only for a discrete number of cases. We use a subroutine which interpolates their results and computes also the number of secondary electrons ejected from helium atoms, Φ_{He}, assuming that Φ_{He}/Φ_H is the same as at higher energies. A similar assumption is used for the fractional energy of the primary which goes into Lyman-α excitation for hydrogen (which will be relevant in computing subthermal effects). We introduce the following symbols:

$f_1(T_K), f_2(T_K)$ are cooling efficiencies due to impact of neutral hydrogen (f_1) and electrons (f_2) with heavier elements (the contribution of each element has been weighted by its abundance with respect to H).

$f_3(T_K)$ is the cooling efficiency for free-free emission and H I recombinations and $f_4(T_K)$ is the cooling efficiency due to H I impact with free electrons.

x_H, x_{He}, and x_{He2} are the fractional ionization of H I, He I, and He II, respectively.

$h_{He} = 0.1$, $h_C = 1.9 \times 10^{-4}$ are the helium and carbon abundance by number with respect to hydrogen.

α_2 is the H I recombination coefficient excluding captures to the $n = 1$ level (Spitzer 1978).

$\alpha_{He}\, \alpha_{He2}$ are the He I and He II recombination coefficients (Spitzer 1978).

α_C is the total recombination coefficient for C I which we assume to be equal to that of H I and $E_C = 2$ eV is the heat released for each carbon ionization.

γ_H is the H I ionization rate due to collisions with free electrons.

ξ_{a1}, $\Phi_{a1,a2}$, and E_{a1} are, respectively: the numbers of photoionizations per second per atom of type $a1$, the number of secondary electrons created by interaction of type $a2$ atoms with primary electrons coming from photoionization of type $a1$ atoms, and the heat released for each photoionization of type $a1$ atoms. The symbol $a1$ can be H, He, or He2 to indicate H I, He I, and He II atoms, the symbol $a2$ can be only H or He because secondary electrons from He II atoms are not considered. We compute these quantities at $z_{1/2}$ for isotropic background radiations described in § 2, attenuated by the overlaying and underlaying layers of gas.

$n_H \simeq P/\{kT_K(1 + x_H + h_{He} + h_{He}\, x_{He} + h_{He}\, x_{He2} + h_C)\}$ is the volume density of H atoms.

$n_e \simeq n_H(x_H + h_{He}\, x_{He} + h_{He}\, x_{He2} + h_C)$ is the volume density of free electrons.

The ionization equilibrium equations for H and He are then

$$n_e \left(\frac{x_H}{1 - x_H} \alpha_2 - \gamma_H \right) = \xi_H (1 + \Phi_{H,H} + \Phi_{H,He})$$
$$+ \frac{1 - x_{He} - x_{He2}}{1 - x_H} h_{He}\, \xi_{He}$$
$$\times (1 + \Phi_{He,H} + \Phi_{He,He}) + \frac{x_{He}}{1 - x_H} h_{He}\, \xi_{He2}$$
$$\times (1 + \Phi_{He2,H} + \Phi_{He2,He}) \equiv \tilde{\zeta} \quad (8)$$

$$n_e x_{\rm He} \alpha_{\rm He} = (1 - x_{\rm He} - x_{\rm He2})\xi_{\rm He}(1 + \Phi_{\rm He,He}) + \frac{(1 - x_{\rm H})}{h_{\rm He}} \xi_{\rm H} \Phi_{\rm H,He} + x_{\rm He} \xi_{\rm He2} \Phi_{\rm He2,He} \quad (9)$$

$$n_e x_{\rm He2} \alpha_{\rm He2} = x_{\rm He2} \xi_{\rm He2} \, . \quad (10)$$

The right-hand side of equation (8) gives $\tilde{\zeta}$, the total number of ionizations per second for a neutral H atom. If the slab is optically thin to the extragalactic background, equation (8) gives ζ the total number of ionizations per second for an unshielded neutral H atom. For Case A with a lower cutoff at 1.5 keV $\zeta \simeq 1.5 \times 10^{-20}$ H ionizations s^{-1}, while $\zeta \sim 3 \times 10^{-17}$ H ionizations s^{-1} for Case C with $E_c = 0.1$ keV, $s = 2.4$ and $I \simeq 5$. The ionization rate ζ for Case B is about the same as for Case C with $s = 2.4$ and $I \approx 1.2$. In Paper II we shall extend the photon spectrum down to the Lyman edge, 13.6 eV, which results in much larger values for ζ.

The energy equation below describes the balance between the cooling rate and the heating rate per H atom due to photoionizations by extragalactic background photons or to additional local heat sources (E_{nr}):

$$n_{\rm H}\left\{(1 - x_{\rm H}) f_1(T_K) + [f_2(T_K) + x_{\rm H} f_3(T_K) + (1 - x_{\rm H}) f_4(T_K)] \frac{n_e}{n_{\rm H}}\right\} = (1 - x_{\rm H}) E_{\rm H} \xi_{\rm H} + h_{\rm He}(1 - x_{\rm He} - x_{\rm He2}) E_{\rm He} \xi_{\rm He} + h_{\rm He} x_{\rm He2} E_{\rm He2} \xi_{\rm He2} + h_{\rm C} E_{\rm C} \alpha_{\rm C}(T_K) n_e + E_{nr} \, . \quad (11)$$

The left-hand side is the cooling per H atom minus the heat due to carbon ionization. The right-hand side is the heating per H atom due to photoionization of hydrogen and helium plus the nonradiative heating per atom, E_{nr}. To simplify the solution of the above set of equations we set $x_{\rm He2} = 0$ at low temperatures while at high temperatures we omit the cooling function f_1. Given $N_{\rm H\,I}$, P_0, and the spectral index of the background radiation we solve the above equations by expressing $x_{\rm He}$, $x_{\rm He2}$, and P/ξ as functions of $x_{\rm H}$ using three of the four equations given above. For each value of T_K then we need to solve numerically one single equation of type $f(x_{\rm H}) = 0$.

Case A.—Due to the high energies of the incoming photons, and to the low intensity of the radiation (which for this case is fixed) the gas is optically thin with negligible fractional ionization of He II. Solutions of $f(x_{\rm H}) = 0$ are found assuming constant values of $\Phi_{a1,a2}$, E_{a1}, and P. Since the degree of H ionization is low, P is determined only by P_0 and $N_{\rm H\,I}$. We calculate $\Phi_{a1,a2}$ and E_{a1} (which are functions of $x_{\rm H}$) with an iterative procedure. T_K is determined by the value of P/ξ if the heating rate due to H and He photoionization is stronger than that due to carbon photoionization.

Case B.—For each value of T_K we guess a value of E_{nr} and solve iteratively $f(x_{\rm H}) = 0$ to find self-consistent values of $x_{\rm H}$, $\Phi_{a1,a2}$, E_{a1}, and P. The attenuated photon flux (or ξ) required at $z_{1/2}$ can be calculated. But since for this case the incident photon flux is fixed, we know what ξ should be for a given $x_{\rm H}$. We adjust E_{nr} accordingly and repeat the calculation until we get the correct value of ξ.

Case C.—The value of $x_{\rm H}$, found by solving $f(x_{\rm H}) = 0$, determines P/ξ and therefore I. The correct solution is found after a few iterations because the spectral distribution of the extragalactic radiation changes when the parameter I varies with T_K.

For each case we then determine the spin temperature, as described at the beginning of this section.

4. SUBTHERMAL EFFECTS IN THE 21 CENTIMETER EMISSION LINE

If the ionizing flux and the pressure P are moderate or small, the spin temperature T_S is depressed below the gas kinetic value T_K and this subthermal effect increases the 21 cm absorption (see § 5). If flux and pressure were extremely small, T_S could be depressed so drastically as to approach T_R, in which case the observed emission quantity N_B would be much less than the actual column density $N_{\rm H\,I}$. As mentioned in the introduction, "H I edges" are observed at $N_B \sim N_I$ and the question arises whether H I could be "hidden" outside such edges. In other words, could there be regions where $N_{\rm H\,I}$ is only slightly smaller than N_I but $N_B \ll N_{\rm H\,I}$? We now give two arguments, one observational and one theoretical, to show that this is not the case.

We selected a few objects with low 21 cm surface brightness ($N_B < 2 \times 10^{19}$ cm^{-2}) observed as part of outer disks by CS (four in M33 and one in NGC 4631) or as HVC by CTS. These are good candidates for a phenomenon of $N_{\rm H\,I} \gg N_B$. In Figure 2 we show the lower limits to T_S calculated from the absence of 21 cm absorption (we assume a line width of 4 km s^{-1} except for one case in M33 where $T_S > 300$ K and we use 8 km s^{-1}). The curves give the $N_{\rm H\,I}$–T_S relation (see eq. [4]) for each selected object and the thick part of the curves displays the allowed values of $N_{\rm H\,I}$. Since they are all on the vertical portion of the curve, where $T_S \gg T_R$ and $N_{\rm H\,I} \simeq N_B$, we can exclude that strong subthermal effects hold for these cases.

For the lowest extragalactic flux and pressure, namely Case A with $E_c = 1.5$ or 0.5 keV and $P_0/k = 0.1$ cm^{-3} K, we have calculated T_S. These small values of flux and pressure should give the largest difference between N_B and $N_{\rm H\,I}$. Figure 3 shows the N_B–$N_{\rm H\,I}$ relation and we can see that no drastic depressions in the brightness are expected for $N_B > 10^{18}$ cm^{-2} (appreciably smaller than N_I). Therefore this proves again that the surface brightness is still a good indicator of the neutral hydrogen column density where H I edges occur. Our conclusion that H I edges are not due to subthermal effects holds even more strongly if the background spectrum extends down to

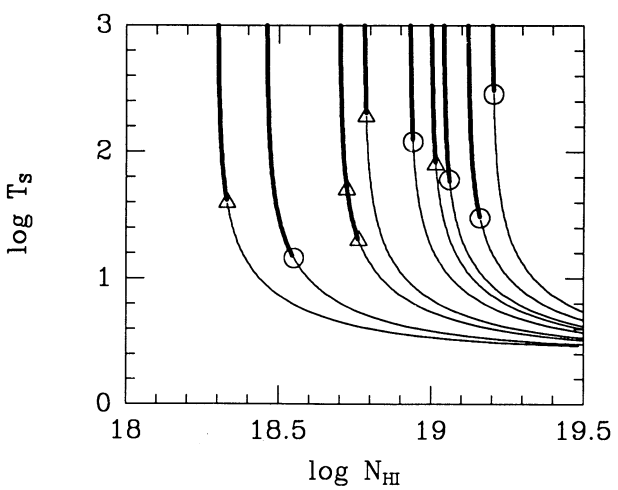

FIG. 2.—T_S–$N_{\rm H\,I}$ relation for all the positive detections of H I with $N_B \leq 2 \times 10^{19}$ cm^{-2} in CS (*circles*) and $N_B \leq 10^{19}$ cm^{-2} in CTS (*triangles*). The thick parts of the curves show the possible pairings of $N_{\rm H\,I}$ and T_S for each data point according to the upper limits obtained from 21 cm absorption data.

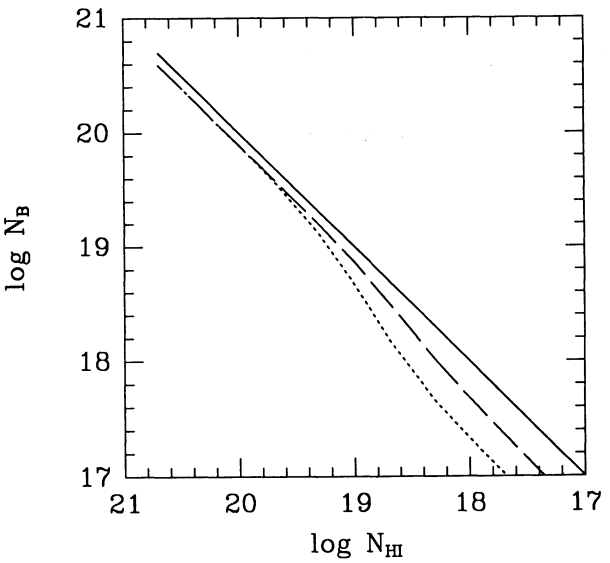

FIG. 3.—Subthermal effects in emission: the column density derived directly from the brightness temperature, N_B, vs. the real $N_{H\,I}$ of the gas. We have used $P_0 = 0.1$ cm^{-3} K, and a low external flux, namely Case A with $E_c = 1.5$ keV (*dotted line*) or $E_c = 0.5$ keV (*dashed line*). The solid line is the line of unity slope in the N_B–$N_{H\,I}$ plane.

lower energies. Table 1 gives $N_{H\,I}/N_B$, T_K and T_S for Case A with $E_c = 1.5$ and 0.5 keV and for a few low values of P_0. Notice that the gas is always in the cold phase and as we increase the pressure T_S approaches T_K, T_K decreases until reaches 12.5 K at very large P_0. This is the lowest possible temperature for our assumed metal abundance and it is reached when heating is provided by carbon ionization. For larger ionizing fluxes (e.g., Case C) we have larger values of T_K and of T_S with a consequent decrease of subthermal effects in emission. Values of T_S in Table 1 are already too large to allow substantial departures of N_B from $N_{H\,I}$, but they are smaller than those observed by CS and CTS (some of which are shown in Fig. 2). This implies extra heat sources in outer regions (Case B) or larger ionizing fluxes than we used for Case A (Case C).

TABLE 1

SUBTHERMAL EFFECTS IN EMISSION—CASE A

$N_B \times 10^{-19}$ (cm^{-2})	P_0/k (cm^{-3} K)	$N_{H\,I}/N_B$	T_K (K)	T_S (K)
	$E_c = 1.5$ keV			
0.1.....	0.1	3.72	13.7	3.7
0.1.....	0.5	2.16	12.9	5.1
0.1.....	1.0	1.75	12.7	6.4
0.1.....	5.0	1.38	12.5	9.9
0.2.....	0.1	2.96	13.3	4.1
0.2.....	0.5	2.08	12.9	5.3
0.2.....	1.0	1.74	12.7	6.4
0.2.....	5.0	1.38	12.5	9.9
0.5.....	0.1	2.10	12.9	5.2
0.5.....	0.5	1.83	12.8	6.0
0.5.....	1.0	1.65	12.7	6.9
0.5.....	5.0	1.38	12.5	9.9
1.0.....	0.1	1.66	12.7	6.9
1.0.....	0.5	1.59	12.6	7.4
1.0.....	1.0	1.54	12.5	7.8
1.0.....	5.0	1.37	12.5	10.1
	$E_c = 0.5$ keV			
0.1.....	0.1	1.94	41.5	5.6
0.1.....	0.5	1.45	22.7	8.9
0.1.....	1.0	1.38	19.2	9.9
0.1.....	5.0	1.30	14.8	11.8
0.2.....	0.1	1.72	35.6	6.5
0.2.....	0.5	1.43	22.4	9.1
0.2.....	1.0	1.37	19.1	10.1
0.2.....	5.0	1.30	14.7	11.9
0.5.....	0.1	1.44	26.2	9.0
0.5.....	0.5	1.38	20.9	10.0
0.5.....	1.0	1.35	18.6	10.6
0.5.....	5.0	1.30	14.7	12.0
1.0.....	0.1	1.34	20.0	10.8
1.0.....	0.5	1.33	18.4	11.1
1.0.....	1.0	1.32	17.3	11.4
1.0.....	5.0	1.29	14.5	12.1

5. THE SPIN TEMPERATURE–HEAT RELATION

The flux assumed in Case A is unrealistically small and implies spin temperatures well below those observed. We confine therefore our attention to Case B and Case C which involve stronger energy inputs to the gas than Case A. In Case B the ionizing flux is fixed, the nonradiative energy input rate E_{nr} varies, and T_S (as well as T_K) are calculated. In Case C, $E_{nr} = 0$ and the intensity of the ionizing flux for $E > 0.1$ keV, I, varies. The results we show are useful for interpreting present and future H I absorption data in terms of heat inputs to the gas from local sources or, in the absence of these, from a cosmic background flux. Using the H I data we have available at the moment, we show that the heat input required from local sources, E_{nr}, is small and compatible with the absence of star formation in outer regions. If there are no local sources (Case C), a comparison between the observed and predicted spin temperature for a given H I column density sets interesting constraints on the intensity of the cosmic background radiation.

We know that for given P and T_K a medium with a lower ionization fraction in the cold phase has a lower cooling rate per atom (Spitzer 1978). This means that for a given T_K Case B requires a heating rate per atom (radiative plus nonradiative) lower than Case C. However, because subthermal effects in Case B are stronger than in Case C, this inequality might not hold for a given T_S. Our results show that even when the external pressure is low and subthermal effects are strong, there is relatively little difference between the heat required in Case B and in Case C for a given T_S. Figure 4 plots E_{nr} versus T_S for Case B in the stable cold and warm phases (solutions requiring $E_{nr} < 0$ have been discarded). For Case C, Figure 5 plots the parameter I in equation (3) versus T_S for $s = 2.4$. Notice that for very small values of I the extragalactic radiation field is unimportant in the energy equation, T_S is constant and determined by the balance between the carbon heating and the line cooling. In Figure 6 we plot T_K versus T_S for all the cases shown in Figures 4 and 5. Notice that the warm phase can start with lower spin temperatures than the final part of the cold phase.

Figures 4 and 5 show E_{nr} or I versus T_S for three different values of $N_{H\,I}$ and two values of the additional pressure P_0. As we increase the parameter P_0, and therefore the density, the heat input (E_{nr} or I) required to reach a certain T_K increases but subthermal effects get smaller and T_S closer to T_K. The result for a given T_S is that E_{nr} or I increases rapidly with P_0 if T_S is

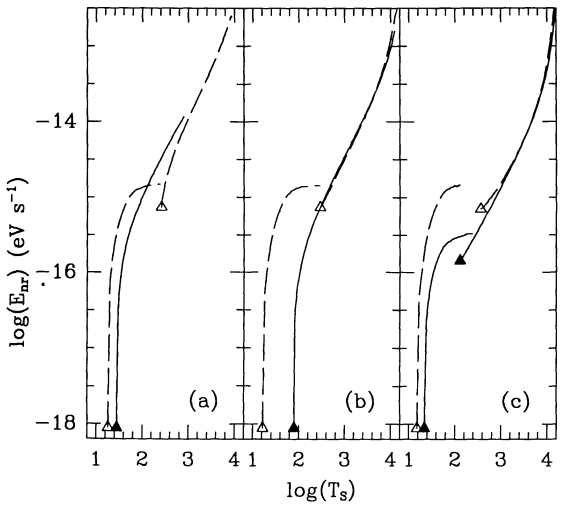

FIG. 4.—Heat per atom required for equilibrium in units of eV s^{-1} for Case B ($E_c = 0.1$ keV, $s = 1.4$, $I = 7.7$). It is shown as function of T_S in the stable cold and warm phases for two values of P_0. The filled triangles indicate the beginning of the two phases when $P_0/k = 1$ cm^{-3} K (*solid lines*) and the open triangles when $P_0/k = 100$ cm^{-3} (*dashed lines*). $N_{HI} = 5 \times 10^{18}$ cm^{-2} in (*a*), 2×10^{19} cm^{-2} in (*b*), and 5×10^{19} cm^{-2} in (*c*).

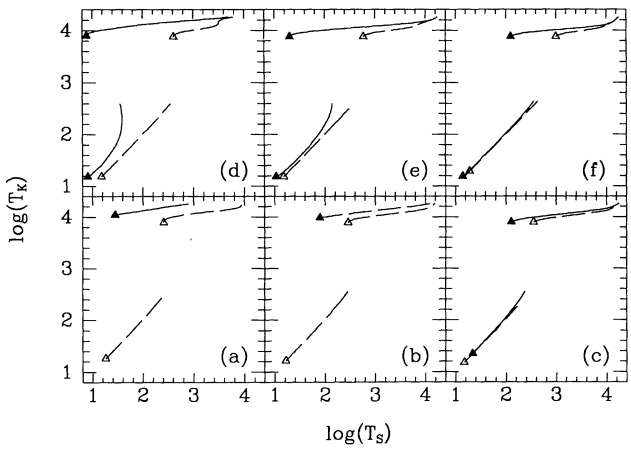

FIG. 6.—T_K–T_S relation for all cases shown in Fig. 4 and in Fig. 5. Case B with (*a*) $N_{HI} = 5 \times 10^{18}$, (*b*) $N_{HI} = 2 \times 10^{19}$, and (*c*) $N_{HI} = 5 \times 10^{19}$ cm^{-2}. For the same values of N_{HI}, (*d*), (*e*), and (*f*) show the T_K–T_S relation for Case C with $s = 2.4$ and $E_c = 0.1$ keV. Lower curves in the panels are for the cold phases, while curves at the top of the panels are for the warm phases.

low. For high T_S the heat input required is almost independent of P_0 and, if the density is not big enough that T_S still differs from T_K, it can decrease with P_0 (see for example Fig. 5 for $T_S \simeq 1000$ K).

For Case C the existence of the cold and/or warm phase of H I depends mainly on the ratio of P (from eq. [7]) to the intensity I: for $P/I < 3k$ there is no cold phase at all, for slightly larger values both phases coexist, and for $P/I > 10k$ there is no warm phase. If the contribution to I from known quasars alone gives $I \sim 5$, the outermost regions of the H I disk, with column densities $N_{HI} \sim 3 \times 10^{19}$ cm^{-2}, are likely to be all in the warm phase when $z_{1/2} \sim 1$ kpc. This should be true even in the absence of E_{nr} or other additional ionizing fluxes (a warm phase with smaller $z_{1/2}$ requires stronger background fluxes). This value of $z_{1/2}$ is what we estimate from Merrifield (1992) for the outermost disk of the Milky Way. Therefore even if the outermost part of galactic H I disks are warm there is no strong evidence for the heat input in outer regions to be much larger than that given by Madau's flux. Figures 4, 5, and 6 show a curious feature for Case B with low heat input ($E_{nr} \lesssim 10^{-15}$ eV s^{-1}) and for Case C with $I \lesssim 10$: the hydrogen is all in the warm phase with $T_K \sim 10^4$ K but the spin temperature is surprisingly low, $T_S \gtrsim 500$ K. Conversely, if observations should give $T_S \gtrsim 1000$ K much larger ionizing fluxes and/or larger E_{nr} would be required.

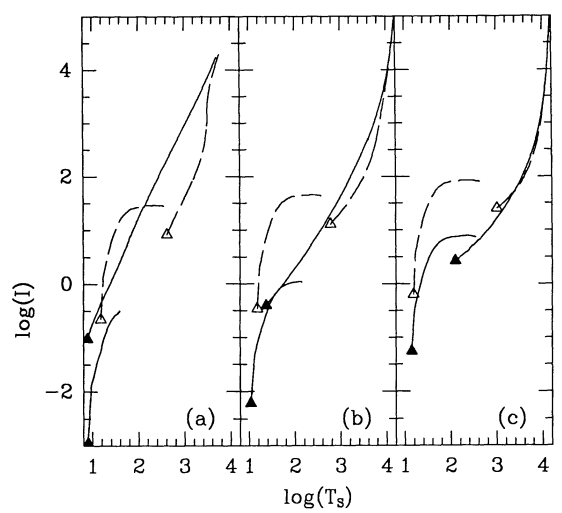

FIG. 5.—Parameter I of the spectrum in eq. (3) as a function of T_S for Case C when $s = 2.4$. The filled triangles indicate the beginning of the cold and warm phase when $P_0/k = 1$ cm^{-3} K (*solid lines*) and the open triangles when $P_0/k = 100$ cm^{-3} K (*dashed lines*). N_{HI} is 5×10^{18} cm^{-2} in (*a*), 2×10^{19} cm^{-2} in (*b*), and 5×10^{19} cm^{-2} in (*c*).

We illustrate the use of Figures 4, 5, and 6 by applying them to the analysis of the observational data for the strongest background source behind the outer disk of M33 (the curve farthest to the right in Fig. 3). Here we have $N_{HI} \simeq N_B \simeq 2 \times 10^{19}$ cm^{-2} along the line of sight, and the absence of absorption gives $T_S > 250$ K (Corbelli & Schneider 1990). The H I surface density perpendicular to the plane will be slightly smaller than the observed value due to the inclination of the outer disk respect to our line of sight (which is less than that of the inner disk but not completely negligible, see Corbelli et al. 1989). Figures 4*b* and 5*b* show that we have possible solutions for both Case B and C with small heat input if P_0 is reasonably small ($P_0/k \lesssim 10$ cm^{-3} K, say). The minimum heat compatible with $T_S \sim 250$ K for small pressures is similar for Case B and C and gives solutions in the warm phase with $E_{nr} \simeq 5 \times 10^{-16}$ eV s^{-1} for Case B and $I \simeq 6$ for Case C with $s = 2.4$ and $E_c = 0.1$ keV. This value of I can be achieved by quasars alone (Madau 1992) and this value of E_{nr} can be supplied by a mild outer galactic fountain (Corbelli & Salpeter 1988). For instance, one requires only 1% of the total in a galaxy supernova energy output rate to flow with energy of $\sim 10^5$ eV cm^{-2} s^{-1} over a disk of 30 kpc radius. If half of this energy is used for heating the disk gas layer below, then $T_S \sim 500$ K for $N_{HI} \approx 2$ or 3×10^{19} cm^{-2}. Slightly smaller spin temperatures are predicted for a gas with lower N_{HI}. To summarize: the present limit of $T_S > 250$ K is still compatible with present estimates of the quasar flux and/or a very mild outer galactic fountain, which are sufficient to keep a gas with $N_{HI} \lesssim 3 \times 10^{19}$ cm^{-2} in the warm phase. The spin temperatures are surprisingly low,

compared to $T_K \sim 10^4$ K (unless the energy input is extremely large).

Another reliable absorption measurement of 21 cm line outside the optical disk is in the spectrum of the quasar 3C 232, at the velocity of the spiral galaxy NGC 3067, close to the quasar on the plane of the sky. The width of this line (Rubin et al. 1982) implies that the absorbing material is H I in its cold phase with $T_S \leq 300$ K and with $N_{\rm H\,I}^{\rm cold} \leq 5.8 \times 10^{19}$ cm^{-2} along the line of sight as derived from the strength of the absorption line. Emission measurements (Carilli & van Gorkom 1992) give a total observed H I column density of $(8 \pm 4) \times 10^{19}$ cm^{-2}; assuming a modest inclination correction factor, it should be $N_{\rm H\,I} \sim 5 \times 10^{19}$ cm^{-2}, so that Figures 4*c* and 5*c* apply. We can be in the narrow range of conditions where the warm and the cold H I phase coexist. If $z_{1/2}$ is of order 1 kpc, as observed in the Milky Way, then $P_0/k \sim 30$ cm^{-3} K; in the vicinity of this pressure Figure 5*c* gives a flux with $I \sim 3(P_0/10k)^{0.5}$ and Figure 4*c* gives for Case B a heating rate $E_{nr} \sim 5 \times 10^{-16}\,(P_0/10k)^{0.3}$ eV s^{-1}. These are only order-of-magnitude relations, but they are compatible with the estimates given above for M33 and with likely quasar fluxes. Figures 4*c* and 5*c* almost make predictions about the warm phase: T_S should be $\sim$300–500 K for Case B and only slightly larger for Case C. More than half of the H I should be in this phase and one might be able to observe a second absorption component with the peculiar combination of a low spin temperature and a large width, $\omega \sim 20$ km s^{-1}, corresponding to the larger T_K.

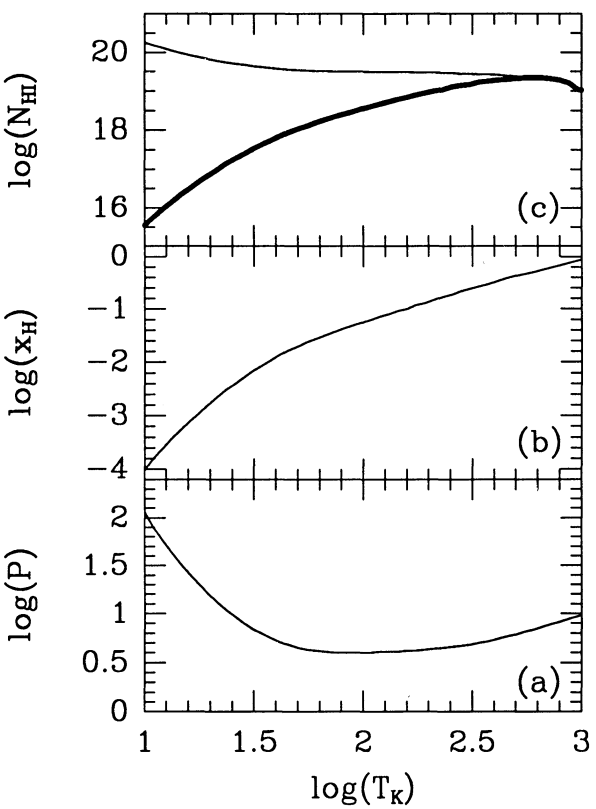

FIG. 7.—In (*a*) and (*b*) we show the pressure and the hydrogen fractional ionization for a gas pervasive of monochromatic photons of 14.6 eV from decaying neutrinos and no other heat sources. The thin and thick curves in (*c*) show the maximum and minimum H I column density, respectively, which are compatible with the corresponding value of T_K (see text for details).

6. DARK MATTER DECAY AND H I TEMPERATURES IN OUTER REGIONS

The dark matter decay theory recently developed by Sciama (Sciama 1990, 1991), predicts a universe populated by heavy neutrinos which decay radiatively producing photons with energy $E_\gamma = 13.6 + \epsilon$ with $\epsilon \sim 1$ eV and a production rate proportional to the density of dark matter. If the local density of the gas is sufficiently high, these photons are produced and absorbed locally and they are the most important photons for the ionization of H I. In the outermost regions of galactic disks the local conditions are very different and the monochromatic photons, both extragalactic and local, can cause a sharp H I edge, even in the absence of quasar photons. This is discussed in Paper II. Here we again consider only the mostly neutral portion of the galactic disk, just inside the edge. We assume first a negligible background flux from quasars and no heat source besides the local neutrino decay photons. Due to the larger number of photons with energy close to 13.6 eV, the Lyman-α pumping will be very effective to bring T_S close to T_K. As source function for these photons we use the expression given by Sciama (1990) for our Galaxy:

$$\phi = \frac{5 \times 10^{-16}}{3 \times (1 + R/R_0)^2}\ \text{cm}^{-3}\ \text{s}^{-1}\,. \tag{12}$$

The equation of state relates density and pressure; the ionization recombination equilibrium and the energy equation in the absence of any external flux are

$$\frac{P x_{\rm H}}{T_K(1 + x_{\rm H} + h_{\rm He})} = \sqrt{\frac{\phi}{\alpha_2}} \tag{13}$$

$$\frac{P}{T_K(1 + x_{\rm H} + h_{\rm He})}\left[\sqrt{\frac{\phi}{\alpha_2}}\, f_1 + (1 - x_{\rm H}) \times \frac{P}{T_K(1 + x_{\rm H} + h_{\rm He})}\, f_2\right] = \phi\epsilon\,. \tag{14}$$

Combining these two equations we have a direct relation between P and T_K, which depends on the square root of the source function ϕ, and on ϵ through $x_{\rm H}$. For $R/R_0 = 3$ Figure 7*a* shows this relation and Figure 7*b* shows the corresponding fractional ionization $x_{\rm H}$. Notice that the gas with low H I column density can survive the external flux in the neutral state only if its pressure is higher than 4 cm^{-3} K; there is also a range of pressures which allows two different equilibrium temperatures. Absorbing the external flux, $F_{\rm ext}$ due to neutrino decay in the halo and in the rest of the universe, requires a column density larger than $N_{\rm min} \equiv 2F_{\rm ext}\, T_K/(P\alpha_2)$, which is plotted as the thick curve in Fig. 7*c*. The thin curve in the same figure shows the maximum column density compatible with a given T_K (obtained by setting $P_0 = 0$). Therefore in the absence of any other heat source $T_K \lesssim 500$ K and the region between the two curves indicates all the possible $N_{\rm H\,I}$–T_K pairs.

If there are extra heat sources in the medium, T_K can be higher than the values shown in Figure 7 and the energy equation will be equation (11) with the helium terms neglected and the heat from a quasar background replaced by the heat from the local monochromatic flux. The nonradiative heat input

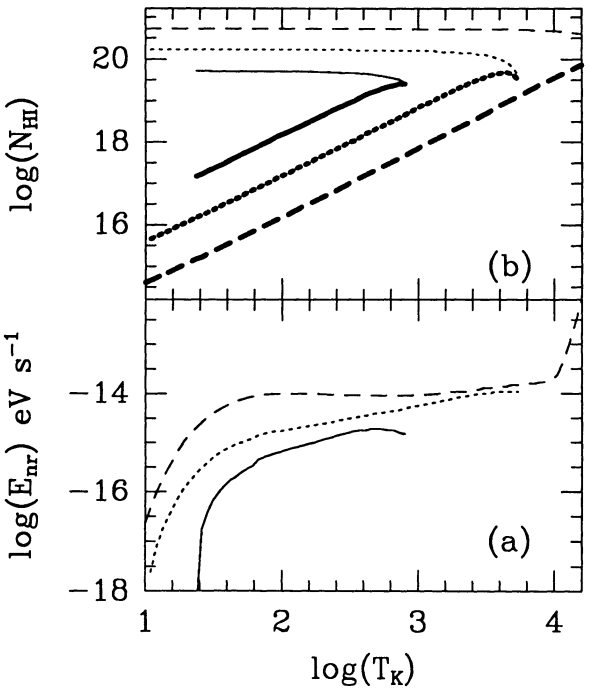

FIG. 8.—In (*a*) the extra heat per atom required by a gas with $P = 10$ (*continuous line*), $P = 100$ (*small dashed line*) and $P = 1000$ (*large dashed line*) cm^{-3} K, is shown as function of the kinetic temperature. In (*b*) thin and thick curves are the maximum and minimum H I column density, respectively, which are compatible with a given value of T_K (see text for details).

which is needed is

$$E_{nr} = \frac{P(1 - x_H)}{T_K(1 + x_H)} f_1 + [f_2 + x_H f_3 + (1 - x_H) f_4] \frac{\phi_\nu}{\alpha_2} - \epsilon\phi \frac{T_K(1 + x_H)}{P}, \quad (15)$$

where $x_H = \sqrt{\phi_\nu/\alpha_2}/(P/T_K - \sqrt{\phi_\nu/\alpha_2})$. E_{nr} depends on N_{HI} only through the pressure term and therefore we can plot E_{nr} versus T_K for several values of P without using P_0 and N_{HI} explicitly. Figure 8*a* shows the E_{nr}–T_K relation for $P/k = 10$, 100, 1000 cm^{-3} K. The extent of the curve is limited by the conditions $E_{nr} > 0$, $0 < x_H < 1$ and $N_{min} < N_{HI} < N_{max}$ (N_{min} and N_{max} being defined as in Fig. 7*c*). For the same values of P, Figure 8*b* shows N_{min} (*thick curves*) and N_{max} (*thin curves*) as function of T_K. Suppose we have gas with $N_{HI} \simeq 2 \times 10^{19}$ cm^{-2} and $T_S > 500$ K; then the minimum required extra heat will be $E_{nr} \simeq 2 \times 10^{-15}$ eV s^{-1} which is comparable to the E_{nr} required for the same column density by Case B, where there are no local monochromatic photons but a background at higher energies. For this case the minimum value of P/k needed for H I survival against the neutrino's external flux is $\simeq 10$ cm^{-3} K. Higher column densities or higher pressures require slightly higher values of E_{nr}. These E_{nr}-values are in reality upper limits since even a modest quasar background, which we have neglected, will contribute somewhat to the heat.

We return now to the two examples of spin temperature measurements. For $N_{HI} \approx 2 \times 10^{19}$ cm^{-2} as in M33, we only have the observational limit $T_S > 250$ K. Figure 7*c* shows that this is compatible with neutrino decay theory even in the absence of extra heat sources. However, for a surface density $N_{HI} \approx 5 \times 10^{19}$ cm^{-2} (as it might be in the case of NGC 3067/3C 232) Figure 7*c* gives $T_S < 30$ K ($T_K \simeq T_S$), whereas the observations showed a higher spin temperature and probably some warm H I. Nonionizing heat sources are therefore required, but E_{nr} need not be larger than for Case B.

7. SUMMARY AND DISCUSSION

In this paper we have discussed H I emission and absorption studies at 21 cm wavelengths which can be used to constrain the spectrum of the extragalactic ionizing radiation below 1 keV, and more generally the rate of heat input outside the optical disk of galaxies. Taking into account self-gravity and considering only unreasonably small lower limit to the extragalactic flux (Case A) we have shown that the number of ionizations and collisions are sufficient to bring the spin temperature well above the background temperature T_R even in the absence of strong compression (due to coronal gas or dark matter). This means that the actual column density, N_{HI}, does not differ appreciably from the value N_B, inferred from the 21 cm brightness temperature at the periphery of galaxies. H I edges observed in outer disks around $N_I \simeq 2 \times 10^{19}$ cm^{-2} (Corbelli et al. 1989; van Gorkom 1991), where N_B drops very rapidly below the minimum detectable value, or the small quantity of HVC gas with $N_{HI} \lesssim 5 \times 10^{18}$ cm^{-2}, correspond then to real cutoffs in the neutral phase of the hydrogen distribution and not to a sudden decrease of the H I spin temperature. These edges are most likely due to ionization by the background radiation and occur when the total gas column density drops below a critical value. This phenomenon will be analyzed in Paper II.

We have carried out model calculations for both the gas kinetic temperature, T_K, and the H I spin temperature, T_S, for various values of gas density and extragalactic background fluxes. We consider a fairly narrow range of hydrogen column densities appropriate to outermost H I disks of spiral galaxies, $N_{HI} \sim (0.5 \text{ to } 5) \times 10^{19}$ cm^{-2}, which are most sensitive to photon energies ~ 0.1 keV. We consider fluxes from below to above the current range of estimates of quasar backgrounds at zero redshifts. As in the classical "two-phase model" we find for these backgrounds $T_K \sim 100$ K for the cold phase and $T_K \sim 10^4$ K for the warm phase. Deviations from thermal equilibrium are still strong and $T_S \ll T_K$ although $T_S \gg 3$ K always. We have carried out calculations both with and without additional nonionizing sources, E_{nr} (to model mild galactic fountains, hydromagnetic waves, etc., traveling from an inner disk to an outer disk). The relationships between E_{nr}, N_{HI}, T_S, T_K, and the intensity I of the background flux are given in Figures 4, 5, and 6.

The models depend not only on the intensity I (for $E_{nr} = 0$), but also on an additional term P_0, with which we estimate the effective compression of the gas (dark matter compression vs. expansion due to some internal nonthermal pressure). If we assume that outermost H I disks with $N_{HI} \sim (2 \text{ to } 5) \times 10^{19}$ cm^{-2} have a vertical scale height $z_{1/2} \sim 1$ kpc, as found for our Galaxy (Merrifield 1992), we obtain $P_0 \sim (10 \text{ to } 30)$ cm^{-3} K. Our models predict that the H I gas in low column density regions should be in the warm phase but the gas in regions with column density of order 5×10^{19} (which have a slightly higher volume density) should be a mixture of cold and warm phases. We analyzed data from an outer region of M33 with $N_{HI} \sim 2 \times 10^{19}$ cm^{-2} where only an upper limit to the absorption was found (Corbelli & Schneider 1990) and one region in NGC 3067 with $N_{HI} \sim 5 \times 10^{19}$ where some absorption was

detected (Carilli & van Gorkom 1992). The nondetection of 21 cm absorption lines through the outer disk of M33, which is a relatively undisturbed H I disk, points out that a significant fraction of the H I gas is warm despite the absence of star-forming regions (in the inner, star-forming disk the fraction of cool H I for M33 is only slightly smaller than for the Milky Way; Dickey & Brinks 1993). This requires a cosmic background stronger than given by the extrapolation of the hard X-ray spectrum down to 0.1 keV. The absorption/emission study for NGC 3067 suggests that both the warm and the cold H I phases are present at the slightly larger column density there.

We found that both observations are compatible with an intensity I of extragalactic photons at energies ~ 0.1 keV roughly as estimated by Madau (1992) for the present-day quasar background. If this extragalactic ionizing flux should turn out to be smaller, one can still explain the observed temperatures by adding a modest amount of nonionizing heat input E_{nr}. Similar heat inputs are required if one replaces the external ionizing flux by monochromatic UV photons produced locally by neutrino decay (Sciama 1990). Only if future observations will show that H I spin temperatures at the periphery of a galaxy are as large as 1000 K would strong local heat sources be required in addition to a QSO ionizing background.

The warm H I phase of the ISM is a dominant component in outermost regions and we can make the following prediction: besides possible narrow H I absorption lines from any cold phase, the warm H I should have a spin temperature still very different from the kinetic one. Values of $T_S \sim 500$ K should be common unless there are heat inputs, either from a background or from local sources, much stronger than what is now believed. This warm phase should produce an absorption line component with quite large width ($\omega \sim 20$ km s^{-1}), which is difficult to detect but would provide an interesting diagnostic because of the $T_S - \omega$ mismatch.

We are grateful to A. Ferrara, C. Giovanardi, R. Reynolds, M. Roberts, S. Schneider, D. Sciama, J. H. van Gorkom, and to the referee for useful comments to the original manuscript. This work was supported in part by NSF grants AST 91-19475, INT 89-13558, and by the Agenzia Spaziale Italiana.

REFERENCES

Bonilha, J. R. M., Ferch, R., Salpeter, E. E., & Slater, G. 1979, ApJ, 233, 649
Bowyer, S. 1991, ARA&A, 29, 59
Brinks, E. 1990, in The Interstellar Medium in Galaxies, ed. H. A. Thronson & J. M. Shull (Dordrecht: Kluwer), 39
Brown, R. L. 1971, ApJ, 164, 387
Carilli, C. L., & van Gorkom, J. H. 1992, ApJ, 399, 373
Carilli, C. L., van Gorkom, J. H., & Stoke, J. T. 1989, Nature, 338, 134
Charlton, J. C., Salpeter, E. E., & Hogan, C. J. 1993, ApJ, 402, 493
Colgan, S. W. J., Salpeter, E. E., & Terzian, Y. 1990, ApJ, 351, 503
Corbelli, E., & Salpeter, E. E. 1988, ApJ, 326, 551
———. 1993, ApJ, 419, 104 (Paper II)
Corbelli, E., & Schneider, S. E. 1990, ApJ, 356, 14 (CS)
Corbelli, E., Schneider, S. E., & Salpeter, E. E. 1989, AJ, 97, 390
Deguchi, S., & Watson, W. D. 1985, ApJ, 290, 578
Dickey, J. M., & Brinks, E. 1993, ApJ, 405, 153
Ferriere, K. M., Zweibel, E. G., & Shull, J. M. 1988, ApJ, 332, 984
Field, G. B. 1958, Proc. I. R. E., 46, 240
Giovanelli, R. 1980, AJ, 85, 1155
Giovanelli, R., & Haynes, M. P. 1988, in Galactic and Extragalactic Radio Astronomy, ed. G. L. Verschuur & K. I. Kellerman (New York: Springer), 522
———. 1991, ApJ, L5
Hartwick, F. D. A., & Schade, D. 1990, ARA&A, 28, 437
Hasinger, G., Schmidt, M., & Trumper, J. 1991, A&A, 246, L2
Heiles, C. 1987, ApJ, 315, 555
Hoffman, G. L., Lu, N. Y., Salpeter, E. E., Farhat, B., Lamphier, & Roos, T. 1993, AJ, submitted
Ibañez, S. M. H., & di Sigalotti, L. 1984, ApJ, 285, 784
Knapp, G. R. 1990, in The Interstellar Medium in Galaxies, ed. H. A. Thronson & J. M. Shull (Dordrecht: Kluwer), 3
Kulkarni, S. R., & Heiles, C. 1988, in Galactic and Extragalactic Radio Astronomy, ed. G. L. Verschuur & K. I. Kellerman (New York: Springer), 95
MacLow, M. M., & McCray, R. 1988, ApJ, 324, 776
Madau, P. 1992, ApJ, 389, L1
Martin, C., & Bowyer, S. 1990, ApJ, 350, 242
McCammon, D., & Sanders, W. T. 1990, ARA&A, 28, 657
McKee, C. F., & Ostriker, J. P. 1977, ApJ, 218, 148
Melott, A. L., McKay, D. W., & Ralston, J. P. 1988, ApJ, 324, L43
Merrifield, M. R. 1992, AJ, 103, 1552
Osterbrock, D. E. 1989, Astrophysics of Gaseous Nebulae and Active Galactic Nuclei (Mill Valley, CA: University Science Books)
Reynolds, R. J. 1990, ApJ, 348, 153
Rubin, V. C., Thonnard, N., & Ford, K. W. 1982, AJ, 87, 477
Sargent, W. L. W., Young, P. J., Boksenberg, A., Carswell, R. F., & Whelan, J. A. J. 1979, ApJ, 230, 49
Schneider, S. E., & Corbelli, E. 1993, ApJ, 414, 500
Schneider, S. E., et al. 1989, AJ, 97, 666
Schwartz, D. A. 1978, in X-ray Astronomy, ed. W. A. Baity & L. E. Peterson (Oxford: Pergamon), 453
Schwartz, D. A., & Tucker, W. H. 1988, ApJ, 332, 157
Sciama, D. W. 1990, ApJ, 364, 549
———. 1991, A&A, 245, 243
Shanks, T., Georgantopoulos, I., Stewart, G. C., Pounds, K. A., Boyle, B. J., & Griffiths, R. E. 1991, Nature, 353, 315
Shull, J. M., & Van Steenberg, M. E. 1985, ApJ, 298, 268, 508
Smith, F. J. 1966, Planet. Space Sci., 14, L71
Spitzer, L. 1942, ApJ, 95, 329
———. 1978, Physical Processes in The Interstellar Medium (New York: Wiley)
van Gorkom, J. H. 1991, in Proc. 3d Haystack Obs. Conf. on Atoms, Ions, and Molecules, ed. A. D. Haschick & P. T. P. Ho (ASP Conf. Ser., 16), 1
Wakker, B. P., Vijfschaft, B., & Schwarz, U. J. 1991, A&A, 249, L5
Wu, X., & Anderson, S. F. 1992, AJ, 103, 1
Wu, X., Hamilton, T. T., Helfand, D. J., & Wang, Q. 1991, ApJ, 379, 564